


Visuospatial processing in early brain-based visual impairment is associated with differential recruitment of dorsal and ventral visual streams

Zahide Pamir ^{1,2}, Claire E. Manley³, Corinna M. Bauer⁴, Peter J. Bex⁵, Daniel D. Dilks⁶, Lotfi B. Merabet^{3,*}

¹Department of Psychology & Department of Neuroscience, Bilkent University, Üniversiteler, Çankaya/Ankara 06800, Turkey

²Aysel Sabuncu Brain Research Center, Bilkent University, Üniversiteler, Çankaya/Ankara 06800, Turkey

³The Laboratory for Visual Neuroplasticity, Department of Ophthalmology, Massachusetts Eye and Ear, Harvard Medical School, 20 Staniford Street, Boston, MA 02114, USA

⁴Lab for Neuroimaging and Vision Science, Department of Radiology, Massachusetts General Hospital, Harvard Medical School, 125 Nashua St. Suite 660, Boston, MA 02114, USA

⁵The Translational Vision Laboratory, Department of Psychology, Northeastern University, 105-107 Forsyth St #125, Boston, MA 02115, USA

⁶Department of Psychology, Emory University, 36 Eagle Row, Atlanta, GA 30322, USA

*Corresponding author: Associate Professor of Ophthalmology, Massachusetts Eye and Ear, Harvard Medical School, 20 Staniford Street, Boston, MA 02114, USA. Email: lotfi_merabet@meei.harvard.edu

Visuospatial processing impairments are prevalent in individuals with cerebral visual impairment (CVI) and are typically ascribed to “dorsal stream dysfunction” (DSD). However, the contribution of other cortical regions, including early visual cortex (EVC), frontal cortex, or the ventral visual stream, to such impairments remains unknown. Thus, here, we examined fMRI activity in these regions, while individuals with CVI (and neurotypicals) performed a visual search task within a dynamic naturalistic scene. First, behavioral performance was measured with eye tracking. Participants were instructed to search and follow a walking human target. CVI participants took significantly longer to find the target, and their eye gaze patterns were less accurate and less precise. Second, we used the same task in the MRI scanner. Along the dorsal stream, activation was reduced in CVI participants, consistent with the proposed DSD in CVI. Intriguingly, however, visual areas along the ventral stream showed the complete opposite pattern, with *greater* activation in CVI participants. In contrast, we found no differences in either EVC or frontal cortex between groups. These results suggest that the impaired visuospatial processing abilities in CVI are associated with differential recruitment of the dorsal and ventral visual streams, likely resulting from impaired selective attention.

Key words: cerebral visual impairment; CVI; fMRI; visual search; naturalistic stimuli.

Introduction

The ability to search for and find an object on a cluttered desk or a person in a crowd is a seemingly effortless, yet essential, function we carry out in our daily activities. For individuals with early brain-based visual impairment, specifically cerebral visual impairment (CVI), both clinical reports and empirical research have revealed that such visuospatial tasks can be particularly difficult, even in cases when visual acuity and visual field functioning are at normal or near normal levels (Boot et al. 2010; Dutton 2013; Dutton et al. 2006; Dutton et al. 2004; Jacobson et al. 1996; Lam et al. 2010; Manley et al.; Manley et al. 2022; McDowell and Dutton 2019). As such, a conceptual framework termed “dorsal stream dysfunction” (DSD; [Dutton 2009; Macintyre-Beon et al. 2010]; see also “dorsal stream vulnerability” [Braddick et al. 2003]) has been proposed to describe the common prevalence of visuospatial impairments (including impaired visual search as just described, as well as deficits in complex motion processing and spatial awareness of surroundings) and their purported association with impaired processing along the dorsal visual stream. Consistent with this view, a previous study by our group demonstrated that individuals with CVI had significantly higher global motion coherence thresholds compared to neurotypical controls in determining the direction of motion (a dorsal stream task

[Pamir et al. 2021]). Furthermore, using fMRI, we found reduced activation in hMT+ (a region in the dorsal stream involved in complex motion processing) compared to controls, while activation in primary visual cortex was comparable between the two groups (Pamir et al. 2021). These findings highlight the role of the dorsal stream in impaired motion processing in CVI, which is not attributed to early visual processing, and support the proposed DSD in CVI hypothesis. Relatedly, in another recent behavioral study, we compared global motion and form coherence thresholds as indices of dorsal and ventral stream functions, respectively. We found that compared to controls, CVI participants showed significantly higher global motion coherence thresholds, while form coherence thresholds were comparable between the two groups (Merabet et al. 2023), suggesting impaired dorsal stream function yet spared ventral stream function (see also [Atkinson 2017]). Importantly, a number of other behavioral studies by our group have provided additional evidence for impaired dorsal stream functioning beyond motion processing in CVI. For example, using a classic conjunction search task, we also revealed that CVI participants showed a profile of greater impairment in visual search efficiency as a function of task difficulty (load) as indexed by an increasing number of surrounding distractors in the search array (Manley et al. 2023). Finally, using a virtual reality (VR)-based

naturalistic static visual search task, we found that CVI participants were more impaired than controls in finding a target toy in a box of other toys (Zhang et al. 2022). The results suggest that the impaired behavioral performance associated with dorsal stream functioning is not limited to global motion processing but is also evident in more generalized visuospatial tasks such as visual search.

But are the visuospatial deficits in CVI explained solely by DSD? Even with the above studies suggesting that the visuospatial deficits in CVI may be specific to DSD, no study to our knowledge has collectively examined the multiple cortical regions beyond the dorsal stream, including early visual cortex (EVC), the ventral visual stream, and frontal cortex that may (or may not) be implicated in the visuospatial impairments in this population. Thus, using a visual search task and fMRI, we investigated the potential extended neural bases of the impaired visual search abilities in CVI under naturalistic viewing conditions. More specifically, we compared visual search performance using eye tracking in CVI participants to neurotypical participants while carrying out a naturalistic VR-based visual search task previously used by our group (Manley et al. 2022). In this task, participants are required to search, locate, and pursue a human target walking in a moving crowd. We also investigated the effect of task difficulty (load) on overall performance by manipulating the size of the surrounding crowd (i.e. the number of people serving as distractors). By using a naturalistic visual stimulus, our overarching goal was to better characterize performance in individuals with CVI in a manner that was more aligned with the self-reported challenges they face in real-world settings. We next adapted our task for the fMRI environment to identify the cortical regions associated with the impaired visual search performance in CVI. Here, we focused on characterizing activation profiles within a priori-defined regions of interest (ROIs), including regions composing EVC, regions along the dorsal (parietal cortex) and ventral (temporal cortex) streams, and frontal cortex.

Dovetailing with the clinical accounts and the previous studies by our group, we found that visual search performance was impaired in CVI participants compared to neurotypicals. Furthermore, fMRI revealed significantly reduced activation in regions along the dorsal stream in CVI compared to neurotypicals, consistent with the DSD in CVI hypothesis. Intriguingly, however, regions along the ventral stream showed the opposite response profile with greater activation compared to neurotypicals, with task difficulty disproportionately affecting the CVI participants. Finally, activation within EVC and frontal cortex was not significantly different between the two groups.

Materials and methods

Study participants

Fourteen (14) individuals with CVI (8 males, mean age = 19.57 years \pm 5.26 SD) and 16 individuals with neurotypical development (5 males, mean age = 22.63 years \pm 3.40 SD) participated in the study (The study size was determined using a prior fMRI study conducted by our group¹⁴). There were no significant differences with respect to age [$t(28) = 1.859$, $P = 0.077$, $d = 0.700$] or the distribution of males/females ($X^2(1) = 2.039$, $P = 0.153$) between the two groups.

All participants with CVI were previously diagnosed by eyecare professionals with extensive clinical experience working with this population (see [Merabet et al. 2023] for further details regarding the diagnosis of CVI). Briefly, the diagnosis was based on a directed and objective assessment of visual functions (including visual acuity, contrast, visual field perimetry, color, and ocular]motor

functions), functional vision assessment (use of structured questionnaires, surveys, and activities), a thorough refractive and ocular examination, as well as an integrated review of medical history and available neuroimaging and electrophysiology records ([Fazzi et al. 2007; Chandna et al. 2021], see also [Boonstra et al. 2022]). Causes of CVI were diverse and included hypoxic-ischemic injury related to prematurity and complications occurring at childbirth, periventricular leukomalacia (PVL), as well as genetic and metabolic disorders. Five CVI participants were born prematurely (i.e. less than 37 weeks gestation). Associated neurodevelopmental comorbidities included cerebral palsy (CP) and a history of developmental delays (according to the definition: “slow to meet or not reaching milestones in one or more of the areas of development including communication, motor, cognition, social-emotional, or adaptive skills expected for the child’s age”; Individuals with Disabilities Education Act, 2004, <https://sites.ed.gov/idea/about-idea/>). Best corrected binocular visual acuity ranged from 20/15 to 20/70 Snellen (or -0.12 to 0.54 logMAR equivalent). Participants with CVI were also categorized according to functional criteria (Dutton and Lueck 2015). In this study sample, 12 out of 14 CVI participants were categorized as category 3 (defined as “functionally useful vision and who can work at or near the expected academic level for their age group”) and the remaining two as category 2 (defined as “have functionally useful vision and cognitive challenges”). Exclusion criteria included any evidence of oculomotor apraxia (i.e. failure of saccadic initiation), intraocular pathology (other than mild optic atrophy), uncorrected strabismus, as well as hemianopia or a visual field deficit corresponding to the area of testing (see Table 1 for complete demographic details). Comparative neurotypicals had normal or corrected-to-normal visual acuities and no previous history of any ophthalmic (e.g. strabismus, amblyopia) or neurodevelopmental conditions.

All study participants had visual acuities, intact visual field function within the area corresponding to the visual stimulus presentation, and fixation and binocular ocular motor function sufficient for completing the task requirements and eye tracking calibration (see Section 2.2 below).

Prior to data collection, written informed consent was obtained from all participants and a parent/legal guardian (in the case of a minor). The study was approved by the Investigative Review Board at the Massachusetts Eye and Ear in Boston, MA, USA, and carried out in accordance with the Code of Ethics of the World Medical Association (Declaration of Helsinki) for experiments involving humans.

Visual stimulus, behavioral task, and analysis of gaze behavior

We assessed visual search performance using a VR-based dynamic human search task previously developed by our group called the “virtual hallway” task (designed using the Unity Technologies 3D game engine v. 5.6; for complete details see [Bennett et al. 2018; Bennett et al. 2021]). Briefly, the task represents a simulated rendering of a hallway of a fictitious school with a crowd of people walking toward and past the observer (Fig. 1A). The scene was presented in a dynamic, continuous fashion, and viewed from a fixed, first-person perspective. Participants were instructed to search, locate, and then pursue the target (the principal, a Caucasian female) walking in the crowd as soon as she appeared from one of eight possible entrances and follow her until she was no longer visible on the screen. The interval between the target disappearing and reappearing in the hallway from trial to trial varied between 5 and 15 s. The duration of the target’s visibility was primarily determined by its starting

Table 1. CVI participant demographics.

Participant ID	Etiology; Comorbidities	Age (years)	Sex	Preterm/Term	Binocular Visual Acuity (Snellen)	Binocular Visual Acuity (LogMAR)	Functional Classification	Global (Total) Lesion Score (n/48)
1	in-utero stroke; cerebral palsy	14	female	preterm	20/25	0.10	3	0.5
2	ischemic hypoxic ischemia	23	female	preterm	20/40	0.30	3	3.5
3	meningitis, infarct	20	female	term	20/40	0.30	3	8.5
4	perinatal head injury, hypoglycemia, anoxia	12	female	term	20/20	0.00	3	4
5	birth complication	20	female	term	20/15	-0.12	3	7.5
6	decreased placental perfusion; global developmental delay	23	female	term	20/70	0.54	3	1
7	focal cortical atrophy; seizure disorder	21	male	term	20/40	0.30	3	16
8	unspecified; developmental delay	22	male	preterm	20/25	0.10	2	2.5
9	genetic disorder	18	male	term	20/20	0.00	3	4
10	unspecified; developmental delay	17	male	term	20/25	0.10	3	2
11	periventricular leukomalacia; cerebral palsy	16	male	term	20/20	0.00	3	16.5
12	periventricular leukomalacia; cerebral palsy	31	male	preterm	20/50	0.40	2	27
13	cystic periventricular leukomalacia; cerebral palsy	11	male	preterm	20/30	0.17	3	14
14	periventricular leukomalacia; cerebral palsy	25	male	preterm	20/25	0.10	3	26

point and path length and varied between 5 and 17 s for the closest and furthest start points, respectively. The primary manipulation of interest was the number of people in the crowd (i.e. distractors), which ranged from 1 to 20 individuals. Task difficulty (load) was categorized as low (average of 5 ± 5 people), medium (10 ± 5), and high (15 ± 5), with each level of crowd density presented equally and in a pseudorandom fashion. For each level of task difficulty, participants experienced an equal number of trials for all possible starting locations of the target. Each run lasted approximately 3.5 minutes and participants completed 3 runs of the experiment with a brief rest period in between. The total testing time was approximately 15 to 20 min for each participant.

Participants were seated comfortably in front of the visual display, and the visual stimulus was presented on a 27-inch monitor (BenQ, 144 Hz refresh rate, 1920×1080 resolution). At a viewing distance of 50 to 60 cm, the scene subtended 58 to 68×32 to 38 degrees of visual angle. Visual search patterns (corresponding to the X and Y coordinate positions of gaze on the screen) were captured using a Tobii 4C Eye Tracker system (90 Hz sampling frequency, Tobii Technology AB, Stockholm, Sweden) mounted on the lower portion of the monitor. Participants were reminded to maintain their gaze on the screen during testing but otherwise could move their heads freely. Prior to data capture, eye tracking calibration was performed on each participant (Tobii Eye Tracking Software, v 2.9 calibration protocol), which took less than one minute to complete. The process included a 7-point calibration task (screen positions: top-left, top-center, top-right, bottom-left, bottom-center, bottom-right, and center-center) followed by a 9-point post calibration verification (i.e. the same 7 calibration points plus center-left and center-right positions). The accuracy criterion was determined by gaze fixation falling within a 2.25 arc degrees radius around each of the 9 points and was further confirmed by visual inspection prior to commencing data collection.

Visual search performance was analyzed based on captured eye-tracking data while participants initially searched, located, and then fixated/followed the target. Two primary objective outcomes were collected for this purpose. Mean success rate (expressed as a percent of correct responses) was defined by whether the participant was able to locate and maintain their pursuit of the target. A trial was considered unsuccessful if a participant failed to locate and establish pursuit for 400 ms prior to the target leaving the screen (end of the trial). A percentage was then calculated based on the condition level of a given trial, and an average of the total number of trials was extracted. Mean reaction time (expressed in ms) was defined as the first moment the participant's gaze arrived within the outer contour of the target and pursued the target on the screen for a given trial. A successful pursuit was defined as gaze that remained within the outer contour of the target for a minimum of 400 ms. In the case where the target entered the hallway and was partially occluded from view, the first moment they became visible to the viewer would mark the start of the reaction time calculation (Bennett et al. 2018; Bennett et al. 2021).

Two secondary outcomes were also analyzed to further characterize search performance. Gaze error (expressed in arc degrees) was defined as the distance between the center of the target and the participant's gaze position. This measure was calculated based on the sampling rate of the eye tracker (90 Hz) and served as a continuous measure of the overall locating and pursuit accuracy of the target stimulus (Bennett et al. 2018; Bennett et al. 2021). Next, visual search area (expressed as a percent of screen area) was determined based on an ellipse-shaped 95% confidence interval fitted to the captured eye tracking data. This measure

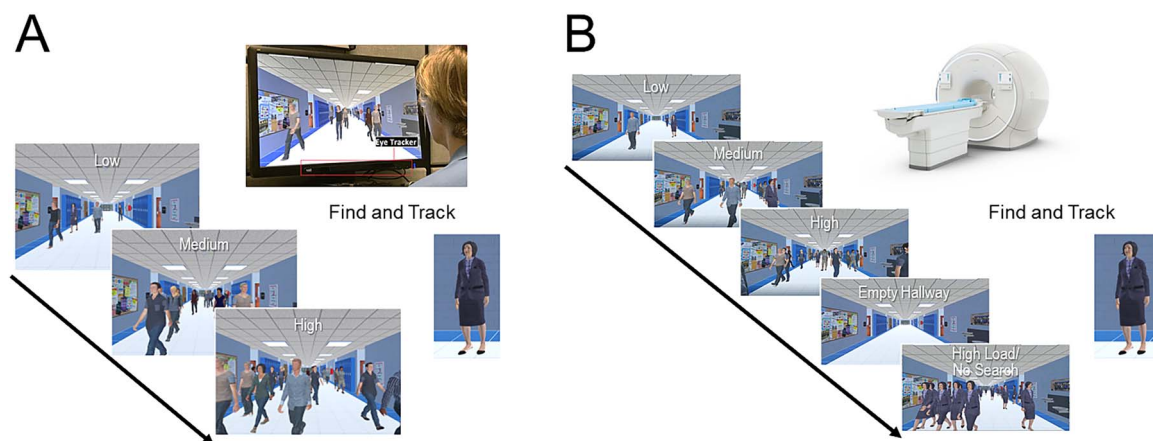


Fig. 1. The virtual hallway task design for the (A) behavioral and (B) fMRI studies. (A) Participants were instructed to search, locate, and pursue a target (the principal) walking in a hallway of a fictitious school. Gaze behavior was recorded using an eye tracker placed below the presentation screen. Task difficulty (load) was manipulated by varying the number of individuals (i.e. distractors) in the crowd, ranging from 1 to 20 people (categorized as low, medium, and high levels of task difficulty). (B) for the fMRI experiment, the behavioral task was the same but with two additional conditions: 1) an empty hallway condition, used as a baseline, and 2) a high load/no search condition, where all the individuals walking in the corridor were identical to the target, used as a control task to isolate visual search from general motion processing see text for further details).

was expressed as a percentage of screen area and represents a measure of visual search precision. Specifically, the ellipse area extended around the perceived centroid location of the target and indicated how well a person searched and continued pursuit within the area they perceived the target to be (precision around spatial centroid). Thus, this measure includes both components of the visual search and pursuit processes (Bennett et al. 2018; Bennett et al. 2021).

Finally, we also determined how often/long participants were able to maintain their gaze within the area of the screen based on the continuous recording of eye gaze coordinate positions. For this purpose, off-screen performance (expressed as a percent) was calculated based on the proportion of gaze points that fell outside of the bounds of the screen on each trial. Given the known frequency of gaze data acquisition (90 Hz), each off-screen data point could be expressed as the specific amount of time, and this outcome served as an index of testing compliance and reliability (Bennett et al. 2018; Bennett et al. 2021).

Statistical analyses were carried out using SPSS Statistics package version 24 (IBM; Armonk, NY, USA). A nonparametric analysis was pursued following confirmation that behavioral data were not normally distributed and that variances were nonhomogeneous (Shapiro–Wilk test). To investigate group differences in performance, a series of initial Mann–Whitney *U* tests followed by a Bonferroni correction for multiple comparisons (adjusted alpha threshold of 0.01) was performed on all outcomes of interest. The effect of task difficulty (load) was evaluated using a Friedman’s test across the two groups. To examine the effect of task difficulty in each group separately, we fitted a least-squares error function to the behavioral data, which consisted of three data points representing the low, medium, and high load task conditions. For this purpose, we used the “polyfit” function in MATLAB (MathWorks, Inc) and calculated the slope of each fitted function. To examine whether increasing task difficulty affected performance in each group, we conducted a Wilcoxon signed-rank test to determine if the median of the slope was different from zero (i.e. a positive slope value indicates an increase in reaction time with increased task difficulty) for the two groups separately. Furthermore, to investigate if task difficulty affected the performance of the two groups differently, we then compared calculated slope values between the two groups using a two-tailed independent-samples Mann–Whitney *U* test.

For outcomes in which there was a significant group difference in overall performance and a significant difference across task difficulty, separate Mann–Whitney *U* tests were conducted to investigate group differences at each task difficulty condition. Effect sizes for Mann–Whitney *U* tests were reported as *r* (calculated by $r = z/\sqrt{N}$).

Magnetic Resonance Imaging (MRI) data acquisition

Participants underwent an MRI scanning protocol using a 3 T Philips Ingenia Elition X scanner (the Netherlands) and a 32-channel phased array head coil. A 3D T1-weighted scan (TE = 2.9 ms, TR = 6.5 ms, flip angle = 8°, isotropic 1 mm acquired voxel size reconstructed from 0.47 x 0.47 x 1.00 mm voxel size) and 3D-FLAIR (TE = 340 ms, TR = 4800 ms, refocusing angle = 40°, isotropic 1.12 mm acquired voxel size, isotropic 0.74 mm reconstructed voxel size) were acquired. Blood oxygen level-dependent (BOLD) signal measurements were acquired with a T2*-weighted gradient-recalled echo-planar imaging (EPI) multiband imaging sequence with a factor of 4 (TR: 2000 ms; TE: 30 ms; flip angle: 90°; spatial resolution: 3 x 3 x 3 mm; number of slices: 44; slice orientation: axial and covering the entire brain).

Structural MRIs of all the CVI participants ($n=14$) were assessed for brain lesion severity according to a reliable and validated semi-quantitative scale (see [Fiori et al. 2014] for complete details). Briefly, sub-scores from each category were summed to provide a global lesion index score (i.e. sum of hemispheric, subcortical, corpus callosum, and cerebellum sub-scores). With this assessment, a higher score is indicative of greater lesion severity. In our sample of CVI participants, global lesion scores ranged from 0.5 to 27 out of a maximum possible score of 48 (see Table 1 and Supplemental Fig. 1 for individual structural scans and Supplemental Table 1 for the correlation scores between global lesion scores and behavior).

Functional Magnetic Resonance Imaging (fMRI) task and analysis

The virtual hallway task described above was adapted as a block design for the purposes of the fMRI experiment. The overall task design remained the same, and participants were again instructed to search, locate, and click a response button as soon as the

target was found and then follow the target in response to the low, medium, and high task load conditions (Fig. 1B). Participants' responses were collected using an MR-compatible response button box to ensure that subjects remained vigilant throughout the task. In addition to three task difficulty conditions, we added two control conditions for subsequent contrast comparisons. First, an "empty hallway" condition had no walking humans present and served as a baseline to control for activation related to the stimulus environment. For this condition, subjects were instructed to explore the visual scene freely, but no behavioral response was required. Second, a high load/no search condition was added where all the humans walking in the corridor were identical to the school principal (i.e. identical to the target) and at a crowd density equivalent to the high task load condition to ensure that any neural differences in visual search were specific to visual search ability and were not simply due to general motion processing ability. For this condition, participants were instructed to explore and track any target they chose randomly, and no behavioral response was required. Each condition lasted 12 s and was repeated five times in a random order throughout each run. All participants completed up to six runs. Visual stimuli were presented on an MR-compatible LCD monitor (32 inches, resolution: 1920 × 1080, refresh rate: 60 Hz; Invivo Corp. Gainesville, USA) mounted to the back of the scanner bore. Participants viewed the screen from a distance of 120 cm via a mirror (7 × 3 inch) mounted on the head coil.

Analysis of the fMRI data was conducted using FSL software package (FMRIB; <http://fsl.fmrib.ox.ac.uk>). Preprocessing steps for the functional data were completed using FSL FEAT (FMRI Expert Analysis Tool) Version 6.00 and included motion correction using MCFLIRT, slice timing correction, spatial smoothing (5 mm), and high-pass temporal filtering (Gaussian-weighted least-squares straight line fitting, with 90 s cut off). Additional head motion-related artifact removal was done using ICA-AROMA (Pruim et al. 2015). Noise components detected by ICA-AROMA were manually evaluated (Griffanti et al. 2017), and those identified as noise were removed from further analysis. In total, 6 runs (3 runs from a neurotypical subject, and 2 runs from a subject with CVI, and 1 run from another subject with CVI) were excluded from the further analysis due to excessive head motion (above 3 mm) in the scanner. Preprocessed functional data were co-registered with the high-resolution anatomical images using boundary-based registration (BBR), and the data were nonlinearly transformed into standard Montreal Neurological Institute (MNI) 152 space (12 degrees of freedom, warp resolution 10 mm). This nonlinear spatial transformation was chosen due to its enhanced capability in addressing the structural abnormalities observed in participants with CVI, and it enabled us to effectively utilize atlas-based regions of interest (ROIs). Voxel time courses for each subject were fit using a general linear model (GLM) for subsequent statistical analysis. Each experimental condition was modeled by a boxcar regressor matching the condition time course and convolved with a double-gamma hemodynamic response function. Due to practical limitations that prevented extending scanning times for our clinical population with CVI, we were unable to incorporate functional localizer runs as part of the fMRI data acquisition. Therefore, analysis of fMRI activation (BOLD signal) data was limited to a priori-defined ROIs using anatomical masks from a probabilistic atlas (Wang et al. 2015). We specifically chose this atlas because of its probabilistic nature and its suitability for use with clinical populations. Given the possibility of greater morphological variability in the brains of the CVI group, we anticipated higher anatomical and functional

variability in the organization of their visual areas. Utilizing a probabilistic atlas effectively addresses this issue by allowing the selection of voxels that are more likely to be functionally associated with specific visual areas. The ROIs included three subregions composing EVC (i.e. V1, V2, and V3), four regions within the dorsal stream (i.e. the middle temporal area [MT], the medial superior temporal area [MST], intraparietal sulcus [IPS], and superior parietal lobule [SPL]), three regions in the ventral stream (i.e. V4, ventral occipital cortex [VOC] and parahippocampal cortex [PHC]), and one region in frontal cortex (i.e. frontal eye fields [FEF]). Further details regarding the anatomical location of ROIs from the Wang et al. (2015) atlas are presented in the supplementary materials section (See Supplemental Fig. 2). ROI masks included all the voxels belonging to each ROI with a 25% threshold or higher probability.

For statistical analyses, we first computed separate GLM contrasts for the low, medium, high, and high load/no search conditions relative to the empty hallway control condition. For each ROI, BOLD signal from each voxel (computed using unthresholded z-statistics produced by FEAT Second Level Analysis for each contrast) were averaged to create a mean signal intensity value, and further analyses were performed using these values.

Statistical analyses were performed using JASP (Version 0.17.1.0, jasp-stats.org). Between- and within-group differences were compared by conducting a mixed design analysis of variance (ANOVA). First, for each ROI, we averaged the BOLD signal within that ROI's subregions and then evaluated group differences by applying 2 × 4 × 3 mixed-design ANOVA with group (CVI and neurotypicals), ROI, and load (low, medium, high) as factors. Similar to the behavioral data analysis, the effect of task difficulty (load) was evaluated by fitting a least-squares error function to the fMRI load activation profile (activation at the low, medium, and high task conditions) separately for each ROI. From there, the slope of each fitted function was calculated for each group. We compared the slopes between the two groups in each visual area using a two-tailed independent-samples t-test (Bonferroni-corrected, adjusted alpha is 0.0125) to examine whether the task difficulty affected the performance of the two groups differently.

Finally, we explored potential relationships between clinical profile indices and behavioral results from the eye-tracking experiment with fMRI activity. Analysis of potential correlations between behavioral performance and activation did not reveal any significant relationships in any of the ROIs tested. We also examined possible associations between baseline visual acuity in our CVI population and behavioral outcomes (reaction time and success rate) and fMRI BOLD signal activation levels across visual areas. This analysis also did not reveal any statistically significant associations or differences. The details of these analyses are reported as part of the supplementary materials section.

Results

Visual search performance

Overall, participants in the CVI group showed impairment in visual search performance compared to neurotypicals, consistent with the proposed DSD in CVI. For success rate, while the CVI group was numerically less accurate than the neurotypicals (89% correct versus 96% correct, respectively), this difference did not reach significance ($U = 137.50$, $P = 0.28$, $r = 0.22$) (Fig. 2A). In contrast, reaction times were significantly (more than 3 times) longer in the CVI group compared to neurotypicals (median RT for CVI and neurotypicals: 4060 vs. 1262 ms; mean RT for CVI and neurotypicals: 4152 vs. 1326 ms) ($U = 26.00$, $P < 0.001$, $r = -0.76$)

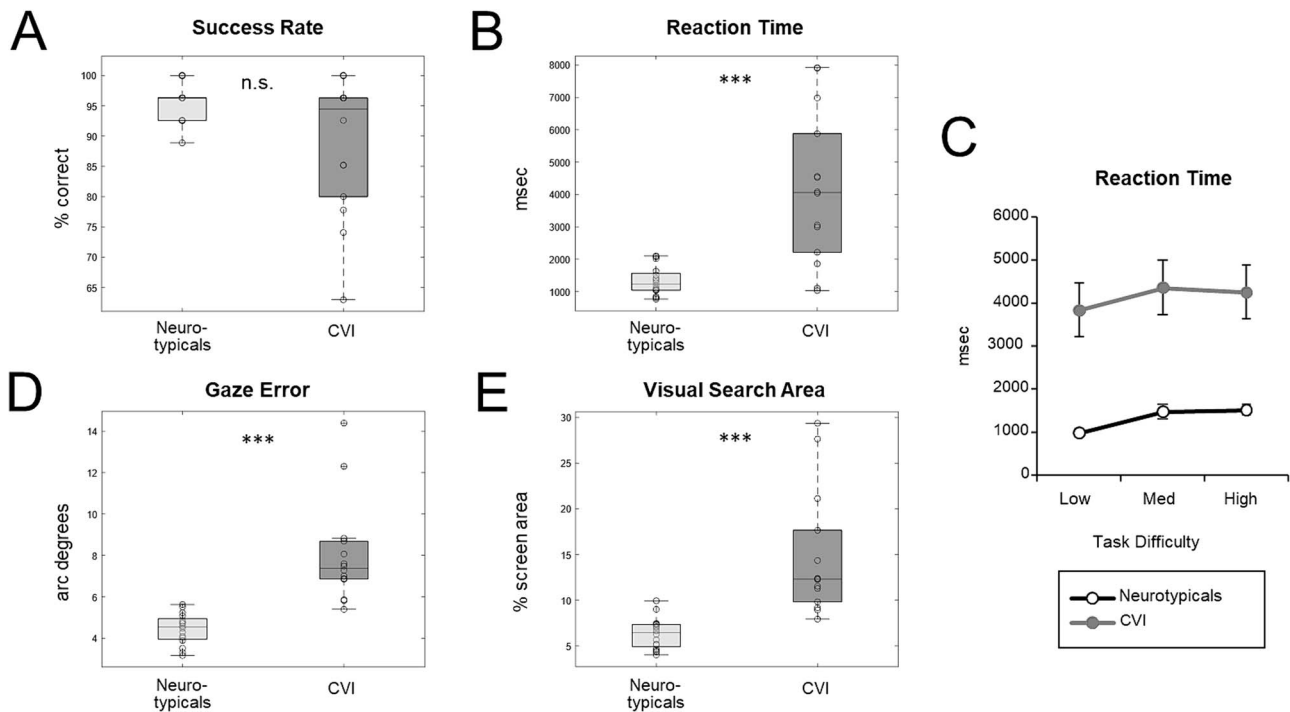


Fig. 2. Visual search performance in CVI and neurotypicals. Individual (circles) and mean (shown as box plots presenting the ranges from the first quartile to the third quartile of the distribution) performance. The line across the bar and whiskers indicate the median and the most extreme data points, respectively). Participants in the CVI group showed an overall impairment in visual search performance compared to neurotypical controls. Although (A) success rate was not significantly different between the two groups, (B) reaction time, (D) gaze error, and (E) visual search area were all significantly higher in the CVI group compared to neurotypicals. (C) Reaction time as a function of task difficulty revealed that increasing task difficulty (load) affected both groups' performance similarly. *** = $P < 0.001$, n.s. = nonsignificant.

(Fig. 2B). Moreover, comparing reaction times as a function of task difficulty between groups (Fig. 2C), we again found a significant difference ($X^2(2) = 22.20$, $P < 0.001$, $W = 0.37$), with post-hoc Mann-Whitney U tests revealing significantly longer reaction times in the low ($U = 33.00$, $P < 0.001$, $r = -0.60$), medium ($U = 27.00$, $P < 0.001$, $r = -0.65$), and high ($U = 21.00$, $P < 0.001$, $r = 0.69$) load conditions in the CVI group, relative to the neurotypicals. Finally, comparing the slope of the fitted functions of the two groups revealed that task difficulty affected both groups similarly ($U = 80.00$, $P = 0.19$, $r = 0.28$). Taken together, these findings reveal that while CVI participants were able to find the target like neurotypicals, they took significantly longer to do so.

Gaze error was also significantly greater in CVI compared to neurotypicals (median gaze error scores for CVI and neurotypicals: 7.38 vs. 4.54 arc degrees; mean gaze error scores for CVI and neurotypicals: 8.03 vs. 4.44 arc degrees) ($U = 2.00$, $P < 0.001$, $r = -0.98$) (Fig. 2D). Next, comparing gaze error as a function of task difficulty by group, we found a significant difference ($X^2(2) = 11.4$, $P = 0.003$, $W = 0.19$), with post hoc Mann-Whitney U tests revealing significantly higher gaze errors in the low ($U = 6.00$, $P < 0.001$, $r = -0.94$), medium ($U = 4.00$, $P < 0.001$, $r = -0.96$), and high ($U = 6.00$, $P < 0.001$, $r = -0.94$) load conditions in CVI, relative to neurotypicals. Moreover, participants in the CVI group searched a greater area compared to neurotypicals (median search area scores for CVI and neurotypicals: 12.3% vs. 6.4% screen area; mean search area scores for CVI and neurotypicals: 14.7% vs. 6.4% screen area) ($U = 6.00$, $P < 0.001$, $r = -0.94$) (Fig. 2E). Next, we compared visual search area as a function of task difficulty and found a significant difference ($X^2(2) = 6.06$, $P = 0.04$, $W = 0.1$), with post-hoc Mann-Whitney U tests revealing significantly greater visual search area in the

low ($U = 6.00$, $P < 0.001$, $r = -0.94$), medium ($U = 7.00$, $P < 0.001$, $r = -0.93$), and high ($U = 15.00$, $P < 0.001$, $r = -0.86$) load conditions in the CVI group, relative to the neurotypicals. Taken together, these results reveal that eye gaze patterns to the target in CVI participants were less accurate and less precise compared to neurotypicals. Note, however, that when comparing off-screen percent values, we found no significant difference between CVI and neurotypicals (median off-screen percent scores for CVI and neurotypicals: 0.18% vs. 0.37%; mean off-screen percent scores for CVI and neurotypicals: 0.65% vs. 0.36%) ($U = 117.501$, $P = 0.83$, $r = 0.09$), revealing that both groups were able to maintain a relatively high level of compliance and engagement in performing the visual search task, and hence cannot explain the significant impairment in our visual search task in CVI.

Functional Magnetic Resonance Imaging (fMRI) activation

To investigate the potential extended neural bases of the above impaired visual search performance in CVI, the main question in this paper, we first collapsed across all subregions within each ROI: i) V1, V2, and V3 composing EVC, ii) MT, MST, IPS, and SPL composing the dorsal stream, and iii) V4, VOC, and PHC composing the ventral stream (note that we only investigated area FEF in the frontal cortex, so there was no need to collapse across subregions). Similar fMRI activations were observed between the right and left hemispheres for both groups across all ROIs except for one visual area within frontal cortex (FEF). Therefore, we analyzed fMRI activation patterns collapsed across hemispheres as part of the main results of this study. The complete results describing hemispheric differences in response

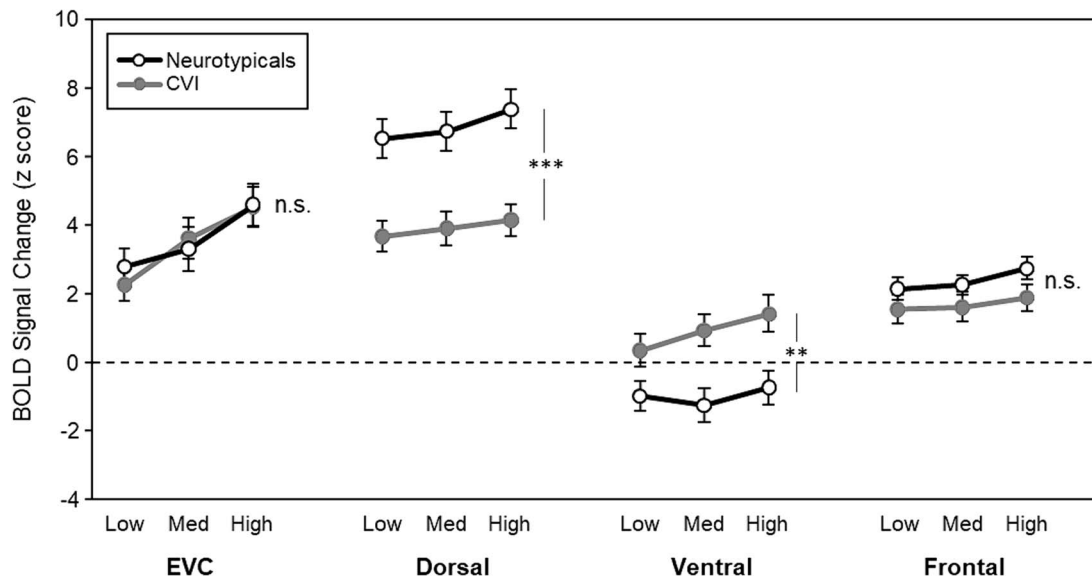


Fig. 3. fMRI activity (BOLD signal) for each ROI as a function of task difficulty by group. Response profiles between the CVI and neurotypical controls were not significantly different in EVC or in frontal cortex. Responses to increasing task difficulty were also not significantly different between groups in these ROIs. In contrast, activity in the dorsal stream ROI was significantly lower for the CVI group compared to the neurotypical controls, while the opposite pattern was found in the ventral stream ROI. Finally, while increasing task difficulty affected both groups similarly in the dorsal stream ROI, the CVI group showed a stronger effect with increasing task difficulty in the ventral stream ROI. Error bars denote standard error of the mean. *** $P < 0.001$, ** $P < 0.01$, n.s. = nonsignificant.

profiles across visual areas are available in the supplementary materials section (See [Supplemental Fig. 3](#)). Next, we ran a 2 (group: CVI, neurotypicals) \times 4 (ROI: EVC, dorsal stream, ventral stream, frontal cortex) \times 3 (task difficulty: low, medium, high) mixed model ANOVA. Critically, we found a significant group by ROI interaction ($F(2.1, 60.7) = 13.2$, $P < 0.001$), indicating that not all ROIs are contributing to the visual search impairment in CVI (Fig. 3). Indeed, Bonferroni corrected pairwise comparisons (adjusted alpha = 0.0125) revealed that activation in both EVC and frontal cortex was not significantly different between groups (EVC: $t(28) = -0.10$, $P = 0.90$; frontal cortex: $t(28) = -1.44$, $P = 0.16$). In contrast, activation in the dorsal stream was significantly lower in the CVI group compared to the neurotypicals ($t(28) = -4.06$, $P < 0.001$), consistent with the proposed DSD in CVI. Activation in the ventral stream was also significantly different between groups ($t(28) = 2.82$, $P = 0.009$), but intriguingly, it was in the complete opposite direction. That is, activation in the ventral stream was significantly higher for the CVI group compared to the neurotypicals. Taken together, these results reveal that the visual search impairment in CVI is associated with differential recruitment of the dorsal and ventral streams and does not involve EVC or frontal cortex.

Finally, there was a significant group by ROI by task difficulty interaction ($F(3.09, 86.7) = 4.91$, $P = 0.003$). Although there was no significant group by task difficulty interaction in the dorsal stream ($F(1.79, 50.24) = 1.39$, $P = 0.25$) and frontal ROI ($F(2, 26) = 0.4$, $P = 0.66$), there was a significant interaction in the ventral stream ROI ($F(1.68, 47.22) = 7.32$, $P = 0.003$), with task difficulty disproportionately affecting the CVI group, relative to the neurotypicals. We also found a marginal difference in the EVC ROI ($F(2, 26) = 3.24$, $P = 0.05$), with task difficulty again disproportionately affecting the CVI group relative to the neurotypicals. However, unlike in the ventral ROI, this difference is most likely due to the increasing amount of visual information across the task difficulty conditions, not task difficulty per se. Indeed, when we directly compared the

ventral ROI to the EVC ROI, we found a significant group by ROI interaction ($F(1, 28) = 8.06$, $P = 0.008$) supporting this idea.

But do the above neural differences in the dorsal and ventral streams really reflect an impairment in visual search in CVI, or could they instead be solely explained by their known impairment in motion processing more generally? To directly address this question, we then compared our high load search task to a control task (i.e. a high load/no search task, matched on motion; see Methods), thus isolating activation related to visual search abilities from motion processing. As a result, any significant increase in fMRI signal would be attributed to carrying out the visual search task. Indeed, Bonferroni corrected pairwise comparisons (adjusted alpha value of 0.0125) showed that fMRI activation related to carrying out the visual search task was greater in EVC ($t(13) = 4.5$, adjusted $P < 0.001$), dorsal ($t(13) = 3.19$, $P = 0.007$), and ventral areas ($t(13) = 3.99$, $P = 0.002$), but not in the frontal area ($t(13) = 1.79$, $P = 0.09$) in the CVI group. However, carrying out the visual search task increased the fMRI activity only in the dorsal ($t(15) = 6.09$, $P < 0.001$) and frontal visual areas ($t(15) = 4.21$, $P < 0.001$), but not in EVC ($t(15) = -1.23$, $P = 0.23$) or ventral areas ($t(15) = 0.84$, $P = 0.41$) in the control group (Fig. 4). Thus, these findings reveal that the neural responses in the dorsal and ventral streams indeed reflect the impairment in visual search performance in CVI and are not only due to their reported impairments related to global motion processing more generally, since both dorsal and ventral streams had significantly greater activation in response to the high load search condition than to the motion-matched high load/no search condition.

Having now established the dorsal and ventral stream contributions to the impairment in visual search in CVI, note, however, that we collapsed across subregions for each ROI; thus, it is still possible that some subregions within either the dorsal or ventral stream may be contributing to the impairment, while others are not. To directly test this possibility, we ran a 2 (group: CVI, neurotypicals) \times 3 (task difficulty: low, medium, high) mixed model

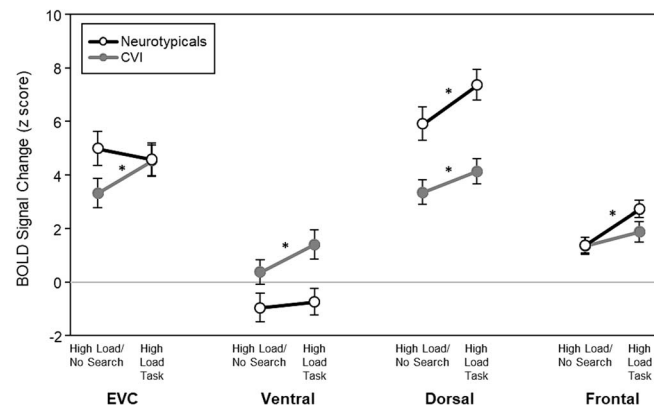


Fig. 4. fMRI activity (BOLD signal) for the visual search task (high load) condition and the high load/no search control condition. Activity in both the dorsal and ventral stream ROIs was significantly lower for the high load/no search task than for the visual search task in CVI. This suggests that neural differences in the dorsal and ventral streams indeed reflect the impairment in visual search in CVI and are not due to their known impairment in motion processing more generally. * $P < 0.01$; Bonferroni corrected for multiple comparisons.

ANOVA for each subregion within the dorsal and ventral stream ROIs separately (Fig. 5). Within the dorsal stream ROI, we found a significant main effect of group in all dorsal stream ROIs, except in IPS, although it displayed a similar trend (MT: $F(1, 28) = 20.16$, $P < 0.001$; MST: $F(1, 28) = 4.65$, $P = 0.04$; SPL: $F(1, 28) = 6.47$, $P = 0.01$; IPS: ($F(1, 28) = 3.65$, $P = 0.06$), revealing that all subregions within the dorsal stream ROI except IPS are contributing to the visual search impairment observed in CVI. Furthermore, no significant group by task difficulty interactions were found in any subregion (MT: $F(2, 56) = 1.84$, $P = 0.17$; MST: $F(1, 28) = 1.44$, $P = 0.24$; IPS: $F(2, 56) = 1.49$, $P = 0.23$; SPL: $F(1.59, 44.75) = 0.58$, $P = 0.52$), revealing task difficulty was processed similarly between groups in all subregions.

Similarly, within the ventral stream ROI, we found a significant main effect of group in V4, VOC, and PHC (V4: $F(1, 28) = 4.65$, $P = 0.04$; VOC: $F(1, 28) = 7.18$, $P = 0.01$; PHC: $F(1, 28) = 9.08$, $P = 0.005$), revealing that all subregions within the ventral stream ROI are contributing to the visual search impairment in CVI. Next, significant group-by-task difficulty interactions were found in some subregions. For V4, the interaction was significant ($F(2, 56) = 3.35$, $P = 0.04$); however, Bonferroni corrected pairwise comparisons showed that the difference between CVI and neurotypicals was not significant for the low, medium, or high load conditions after correcting for multiple comparisons ($P > 0.05$). For VOC, the interaction between group and task difficulty was significant ($F(1.55, 43.6) = 7.06$, $P = 0.004$). Although the difference between CVI and neurotypicals was not significant (adjusted $\alpha = 0.016$) in the low load condition ($t(28) = 2.16$, $P = 0.03$), the difference was significant in the medium ($t(28) = 2.97$, $P = 0.006$) and high load conditions ($t(28) = 2.73$, $P = 0.011$). Finally, for PHC, the interaction between group and task difficulty was also significant ($F(1.49, 41.79) = 5.45$, $P = 0.01$), with a marginal difference between groups (adjusted $\alpha = 0.016$) in the low load condition ($t(28) = 2.3$, $P = 0.02$) and significant differences in the medium ($t(28) = 3.27$, $P = 0.003$) and high load conditions ($t(28) = 3.06$, $P = 0.005$). Finally, to confirm this differential profile of activation within ventral visual areas, we reanalyzed our data using an alternate standard atlas by Glasser et al. (2016) to define ROIs in the ventral stream (Glasser et al. 2016). This additional analysis confirmed evidence of a differential pattern of activity in various ventral stream ROIs between the CVI and control groups (See Supplemental Fig. 4). Taken together, these findings reveal that task difficulty disproportionately affects the CVI group

relative to the neurotypicals, as evidenced by some subregions (i.e. VOC and PHC) in particular.

Discussion

In this study, we asked how cortical regions beyond those in the dorsal stream might contribute to the visuospatial processing impairments observed in early brain-based visual impairment, specifically in individuals diagnosed with CVI. We first confirmed that visual search performance was impaired in CVI participants compared to neurotypicals using a naturalistic VR-based visual search task. Indeed, the CVI participants took longer to find and follow the target, and their eye gaze patterns were less accurate and less precise as compared to neurotypicals. Critically, these observed differences were not explained by differences in overall task engagement between both groups. Next, turning to our main question about how the dorsal stream, as well as other cortical regions, might contribute to this impairment, we found that activity across task difficulty (i.e. load) in the dorsal stream was significantly reduced in the CVI group compared to neurotypicals, consistent with proposed DSD in CVI. However, and somewhat surprisingly, we also found the exact opposite pattern in the ventral stream. That is significantly greater activity in CVI compared to neurotypicals. Furthermore, the CVI group exhibited a greater increase in activity in the ventral stream with increasing task difficulty relative to the neurotypicals. Despite the differential pattern of activity in the dorsal and ventral stream areas, no significant differences in activity were found in either EVC or frontal cortex between groups. Taken together, these results demonstrate that visuospatial processing impairments in CVI are associated with differential recruitment of dorsal and ventral visual streams rather than differences in processing within EVC or frontal cortex.

The result of increased activation in ventral stream areas in CVI compared to neurotypicals was further confirmed by reanalyzing our data using another standard atlas (see the supplementary materials section Supplemental Fig. 4). In our original analysis, we intentionally avoided investigating BOLD activity in specific regions within the ventral stream associated with processing certain stimuli, such as faces or places, for two reasons. First, we did not have a priori hypotheses relating to potential differential patterns of activity within ventral stream areas, nor did we conjecture that any particular ventral stream area would show a differential

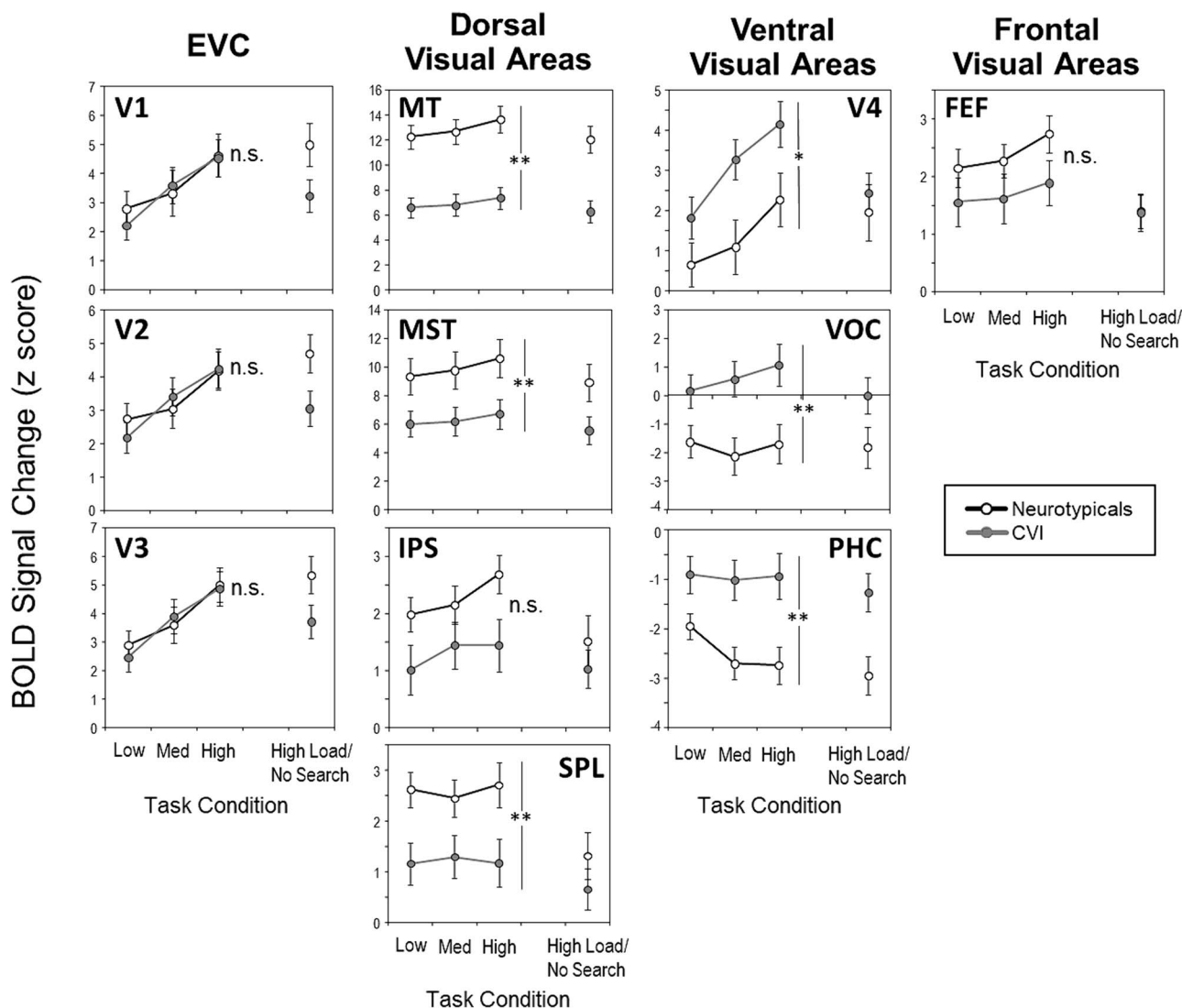


Fig. 5. fMRI activity (BOLD signal) for each subregion within the EVC, dorsal stream, ventral stream, and frontal visual ROIs as a function of task difficulty by group. fMRI activity was consistently lower in the CVI group compared to the neurotypical controls in all subregions within the dorsal stream ROI, while the opposite pattern was observed in subregions within ventral stream. Error bars denote standard error of the mean. *** = $P < 0.001$, ** = $P < 0.01$, * = $P < 0.05$, n.s. = nonsignificant. See text for ROI abbreviations.

pattern of activation compared to others. Second, it is important to realize that the baseline condition we chose was not ideal for describing activation patterns in any particular visual area as scene information was available in both the experimental and baseline conditions. Specifically, information related to biological motion, faces, and body parts was either present in the experimental condition or absent in the baseline condition simultaneously because we did not systematically manipulate any specific visual information in isolation between these two conditions. How visual information processing is affected in CVI, particularly for specific types of stimuli such as faces, objects, places, scenes, and biological motion, still remains to be elucidated. To accurately describe activation patterns within a certain visual area (such as scene-selective areas), future studies should use tailored baseline conditions together with functional localizers.

The behavioral profile of impaired visual search performance is in line with previous studies by our group using similar dynamic VR-based tasks (Manley et al. 2022), static VR-based environments (Zhang et al. 2022), as well as a classic conjunction search task (Manley et al. 2023). Contrary to our previous studies, however,

the ability to find the target in this CVI group was not significantly different compared to neurotypicals (albeit the CVI group was still significantly slower to do so). This apparent discrepant finding is most likely due to methodological differences between this study and our prior ones. For example, presenting the stimulus for a relatively longer time in this study, compared to the prior ones, may have helped the CVI group better engage with the task, and ultimately achieve a success rate that was more comparable to neurotypicals. Moreover, it is possible that the demands related to carrying out both the behavioral and fMRI components of the study placed limitations on recruiting a broad group of CVI participants, which could lead to a potential selection bias in our CVI group compared to the previous studies (see also [Bhat et al. 2021]). Note, however, that these potential methodological differences between this study and the prior ones would only lead to an underestimation in terms of the behavioral and neural differences between CVI and neurotypicals, and thus, future studies investigating a broader group would most likely find similar and possibly even larger effects. Finally, considering that our observed profile of impaired visual search performance in CVI appears

consistent across various tasks (e.g. [Manley et al. 2022; Zhang et al. 2022; Manley et al. 2023]), we would predict that associated fMRI activity patterns (and, in particular, within the dorsal and ventral streams) would generalize to other visual search tasks as well. However, future combined behavioral fMRI studies are needed to confirm this prediction.

So, what then explains the differential recruitment of dorsal and ventral visual streams in CVI during a visual search task? While the exact answer is unclear, two general interpretations could be considered. One intuitive interpretation is that the increased activation in the ventral stream reflects a compensatory mechanism, essentially being “over recruited” to compensate for the impaired dorsal stream. For example, it has been proposed that in the face of decreased white matter integrity, increased neuronal activity may serve to compensate for impaired processing (termed as “less wiring, more firing”; [Daselaar et al. 2015], but see Pamir et al. 2021). However, while this interpretation is appealing, especially since diffusion-based imaging studies find that white matter integrity is compromised in individuals with CVI, these studies find compromised white matter integrity both along the inferior longitudinal fasciculus (ILF; [Ortibus et al. 2012], corresponding to the ventral stream [Ffytche et al. 2010; Rokem et al. 2017]), and along the superior longitudinal fasciculus (SLF; corresponding to the dorsal stream [Bauer et al. 2014]). Thus, decreased white matter integrity along both the ventral and dorsal streams should lead to increased activation in both streams—which we did not find here, instead finding increased activation in the ventral stream and decreased activation in the dorsal stream.

An alternative interpretation then (and the one that we favor) is that the increased activation in the ventral stream yet decreased activation in the dorsal stream reflects impaired top-down suppression of task-irrelevant information, appealing to the biased competition theory (Desimone and Duncan 1995; Beck and Kastner 2009). More specially, we propose that the increased activation in the ventral stream may represent activation driven by bottom-up processing that is “unchecked” by impaired selective attention processing typically provided by the dorsal stream (e.g. IPS and SPL). In agreement with this hypothesis, we also observed negative BOLD signal activation profiles for the control group in the ventral occipital and parahippocampal areas, which are known to be involved in scene processing. While negative BOLD signal activations should be interpreted with caution, this finding aligns with previous reports where suppression of irrelevant sensory processing has been associated with negative BOLD activity (Amedi et al. 2005). Given that the analysis of scene-related information was not crucial for our visual search task and acted more as a distractor, it is possible that it was ignored, particularly at higher levels of task demand (Lavie 2005). Thus, it is possible that control participants were able to more successfully suppress scene-related information, as indicated by their negative BOLD response profiles compared to the CVI group. Furthermore, if increased ventral stream and decreased dorsal stream activation reflect impaired selective attention, we would expect that as the difference between dorsal and ventral activation decreases, visual search performance should correspondingly worsen. This idea is indeed supported by ancillary analysis demonstrating a negative correlation trend between the difference in dorsal and ventral activity and reaction time in the CVI group (see Supplemental Fig. 5). Finally, further anatomical support for the impaired selective attention hypothesis is provided by recent evidence by our group showing reduced integrity of the inferior frontal-occipital fasciculus (IFOF

[Bauer and Merabet 2023]), an important pathway implicated in selective visual attention (Umarova et al. 2010; Chechlacz et al. 2015). In summary, here we found that both the dorsal and ventral streams, but not EVC or frontal cortex, contribute to the known visuospatial impairment in individuals with CVI, suggesting a more complex clinical profile characterizing this condition. A greater understanding of the nature of higher-order visual processing deficits (particularly in the context of naturalistic viewing conditions) is crucial to better characterize the nature of this condition, as well as potentially help devise appropriate rehabilitative strategies for individuals with CVI.

Acknowledgments

The authors would like to thank Christopher Bennett for the initial design of the behavioral task and the subjects and their families for their participation in this study.

Author contributions

Zahide Pamir (Conceptualization, Data curation, Formal Analysis, Investigation, Methodology, Software, Visualization, Writing—original draft, Writing—review & editing), Claire E. Manley (Data curation, Formal Analysis, Project administration, Visualization), Corinna Bauer (Conceptualization, Data curation, Formal Analysis, Investigation, Methodology, Validation, Visualization), Peter J. Bex (Conceptualization, Methodology, Software), Daniel Dilks (Conceptualization, Methodology, Supervision, Writing—original draft, Writing—review & editing), Lotfi Merabet (Conceptualization, Data curation, Funding acquisition, Investigation, Methodology, Project administration, Resources, Supervision, Visualization, Writing—original draft, Writing—review & editing).

Funding

This work was supported by grants from the National Institute of Health/National Eye Institute (NIH/NEI R01 EY030973 to LBM).

Conflict of interest statement: The authors declare no conflict of interest.

Data availability

The data that support the findings of this study are available from the corresponding author upon reasonable request and are subject to IRB approval.

References

- Amedi A, Malach R, Pascual-Leone A. Negative BOLD differentiates visual imagery and perception. *Neuron*. 2005;48(5):859–872. <https://doi.org/10.1016/j.neuron.2005.10.032>.
- Atkinson J. The Davida teller award lecture, 2016: visual brain development: a review of “dorsal stream vulnerability”—motion, mathematics, amblyopia, actions, and attention. *J Vis*. 2017;17(3):26. <https://doi.org/10.1167/17.3.26>.
- Bauer C, Merabet LB. Aberrant white matter development in cerebral visual impairment: a proposed mechanism for visual dysfunction following early brain injury. *J Integr Neurosci*. 2024;23(1):1. <https://doi.org/10.31083/j.jin2301001>. PMID: 38287851.
- Bauer CM, Heidary G, Koo BB, Killiany RJ, Bex P, Merabet LB. Abnormal white matter tractography of visual pathways detected

- by high-angular-resolution diffusion imaging (HARDI) corresponds to visual dysfunction in cortical/cerebral visual impairment. *J AAPOS*. 2014;18(4):398–401. <https://doi.org/10.1016/j.jaapos.2014.03.004>.
- Beck DM, Kastner S. Top-down and bottom-up mechanisms in biasing competition in the human brain. *Vis Res*. 2009;49(10):1154–1165. <https://doi.org/10.1016/j.visres.2008.07.012>.
- Bennett CR, Bailin ES, Gottlieb TK, Bauer CM, Bex PJ, Merabet LB. Assessing visual search performance in ocular compared to cerebral visual impairment using a virtual reality simulation of human dynamic movement. *APA Science*. 2018;4:1–4, 6.
- Bennett CR, Bex PJ, Merabet LB. Assessing visual search performance using a novel dynamic naturalistic scene. *J Vis*. 2021;21(1):5. <https://doi.org/10.1167/jov.21.1.5>.
- Bhat A, Biagi L, Cioni G, Tinelli F, Morrone MC. Cortical thickness of primary visual cortex correlates with motion deficits in periventricular leukomalacia. *Neuropsychologia*. 2021;151:107717. <https://doi.org/10.1016/j.neuropsychologia.2020.107717>.
- Boonstra FN, Bosch DGM, Geldof CJA, Stellingwerf C, Porro G. The multidisciplinary guidelines for diagnosis and referral in cerebral visual impairment. *Front Hum Neurosci*. 2022;16:727565. <https://doi.org/10.3389/fnhum.2022.727565>.
- Boot FH, Pel JJ, van der Steen J, Evenhuis HM. Cerebral visual impairment: which perceptive visual dysfunctions can be expected in children with brain damage? A systematic review [research support, non-U.S. Gov't review]. *Res Dev Disabil*. 2010;31(6):1149–1159. <https://doi.org/10.1016/j.ridd.2jg000.010.08.0010--v>.
- Braddick O, Atkinson J, Wattam-Bell J. Normal and anomalous development of visual motion processing: motion coherence and 'dorsal-stream vulnerability' [research support, non-U.S. Gov't review]. *Neuropsychologia*. 2003;41(13):1769–1784 <http://www.ncbi.nlm.nih.gov/pubmed/14527540>.
- Chandna A, Ghahghaei S, Foster S, Kumar R. Higher visual function deficits in children with cerebral visual impairment and good visual acuity. *Front Hum Neurosci*. 2021;15:711873. <https://doi.org/10.3389/fnhum.2021.711873>.
- Chechlacz M, Gillebert CR, Vangkilde SA, Petersen A, Humphreys GW. Structural variability within Frontoparietal networks and individual differences in attentional functions: an approach using the theory of visual attention. *J Neurosci*. 2015;35(30):10647–10658. <https://doi.org/10.1523/JNEUROSCI.0210-15.2015>.
- Daselaar SM, Iyengar V, Davis SW, Eklund K, Hayes SM, Cabeza RE. Less wiring, more firing: low-performing older adults compensate for impaired white matter with greater neural activity. *Cereb Cortex*. 2015;25(4):983–990. <https://doi.org/10.1093/cercor/bht289>.
- Desimone R, Duncan J. Neural mechanisms of selective visual attention. *Annu Rev Neurosci*. 1995;18:193–222. <https://doi.org/10.1146/annurev.ne.18.030195.001205>.
- Dutton GN. 'Dorsal stream dysfunction' and 'dorsal stream dysfunction plus': a potential classification for perceptual visual impairment in the context of cerebral visual impairment? [comment]. *Dev Med Child Neurol*. 2009;51(3):170–172. <https://doi.org/10.1111/j.1469-8749.2008.03257.x>.
- Dutton GN. The spectrum of cerebral visual impairment as a sequel to premature birth: an overview. *Doc Ophthalmol*. 2013;127(1):69–78. <https://doi.org/10.1007/s10633-013-9382-1>.
- Dutton, GN, Lueck, AH (2015). Impairment of vision due to damage to the brain. In: A. H. L. A. G. N. Dutton (Ed.), *Vision and the brain: understanding cerebral visual impairment in children* (pp. 3–20). AFB Press New York.
- Dutton GN, Saaed A, Fahad B, Fraser R, McDaid G, McDade J, Mackintosh A, Rane T, Spowart K. Association of binocular lower visual field impairment, impaired simultaneous perception, disordered visually guided motion and inaccurate saccades in children with cerebral visual dysfunction—a retrospective observational study. *Eye*. 2004;18(1):27–34. <https://doi.org/10.1038/sj.eye.6700541>.
- Dutton GN, McKillop EC, Saidkasimova S. Visual problems as a result of brain damage in children. *Br J Ophthalmol*. 2006;90(8):932–933. <https://doi.org/10.1136/bjo.2006.095349>.
- Fazzi E, Signorini SG, Bova SM, La Piana R, Ondei P, Bertone C, Misefari W, Bianchi PE. Spectrum of visual disorders in children with cerebral visual impairment. *J Child Neurol*. 2007;22(3):294–301. <https://doi.org/10.1177/08830738070220030801>.
- Ffytche DH, Blom JD, Catani M. Disorders of visual perception [review]. *J Neurol Neurosurg Psychiatry*. 2010;81(11):1280–1287. <https://doi.org/10.1136/jnnp.2008.171348>.
- Fiori S, Cioni G, Klingels K, Ortibus E, Van Gestel L, Rose S, Boyd RN, Feys H, Guzzetta A. Reliability of a novel, semi-quantitative scale for classification of structural brain magnetic resonance imaging in children with cerebral palsy. *Dev Med Child Neurol*. 2014;56(9):839–845. <https://doi.org/10.1111/dmcn.12457>.
- Glasser MF, Coalson TS, Robinson EC, Hacker CD, Harwell J, Yacoub E, Ugurbil K, Andersson J, Beckmann CF, Jenkinson M, et al. A multi-modal parcellation of human cerebral cortex. *Nature*. 2016;536(7615):171–178. <https://doi.org/10.1038/nature18933>.
- Griffanti L, Douaud G, Bijsterbosch J, Evangelisti S, Alfaro-Almagro F, Glasser MF, Duff EP, Fitzgibbon S, Westphal R, Carone D, et al. Hand classification of fMRI ICA noise components. *NeuroImage*. 2017;154:188–205. <https://doi.org/10.1016/j.neuroimage.2016.12.036>.
- Jacobson L, Ek U, Fernell E, Flodmark O, Broberger U. Visual impairment in preterm children with periventricular leukomalacia—visual, cognitive and neuropaediatric characteristics related to cerebral imaging. *Dev Med Child Neurol*. 1996;38(8):724–735. <https://doi.org/10.1111/j.1469-8749.1996.tb12142.x>.
- Lam FC, Lovett F, Dutton GN. Cerebral visual impairment in children: a longitudinal case study of functional outcomes beyond the visual acuities. *Journal of Visual Impairment & Blindness*. 2010;104(10):625–635.
- Lavie N. Distracted and confused?: selective attention under load. *Trends Cogn Sci*. 2005;9(2):75–82. <https://doi.org/10.1016/j.tics.2004.12.004>.
- Macintyre-Beon C, Ibrahim H, Hay I, Cockburn D, Calvert J, Dutton GN, Bowman R. Dorsal stream dysfunction in children. A review and an approach to diagnosis and management. *Curr Pediatr Rev*. 2010;6(3):166–182. <https://doi.org/10.2174/157339610793743895>.
- Manley CE, Bennett CR, Merabet LB. Assessing higher-order visual processing in cerebral visual impairment using naturalistic virtual-reality-based visual search tasks. *Children (Basel)*. 2022;9(8):1114. <https://doi.org/10.3390/children9081114>.
- Manley CE, Bauer CM, Bex PJ, Merabet LB. Impaired visuospatial processing in cerebral visual impairment revealed by performance on a conjunction visual search task. *Br J Vis Impair*. 2023;0(0):02646196231187550. <https://doi.org/10.1177/02646196231187550>.
- McDowell N, Dutton GN. Hemianopia and features of Balint syndrome following occipital lobe Hemorrhage: identification and patient understanding have aided functional improvement years after onset. *Case Rep Ophthalmol Med*. 2019;2019:3864572. <https://doi.org/10.1155/2019/3864572>.
- Merabet LB, Manley CE, Pamir Z, Bauer CM, Skerswetat J, Bex PJ. Motion and form coherence processing in individuals with cerebral visual impairment. *Dev Med Child Neurol*. 2023;65(10):1379–1386. <https://doi.org/10.1111/dmcn.15591>.

- Ortibus E, Verhoeven J, Sunaert S, Casteels I, de Cock P, Lagae L. Integrity of the inferior longitudinal fasciculus and impaired object recognition in children: a diffusion tensor imaging study. *Dev Med Child Neurol*. 2012;54(1):38–43. <https://doi.org/10.1111/j.1469-8749.2011.04147.x>.
- Pamir Z, Bauer CM, Bailin ES, Bex PJ, Somers DC, Merabet LB. Neural correlates associated with impaired global motion perception in cerebral visual impairment (CVI). *Neuroimage Clin*. 2021;32:102821. <https://doi.org/10.1016/j.nicl.2021.102821>.
- Pruim RHR, Mennes M, van Rooij D, Llera A, Buitelaar JK, Beckmann CF. ICA-AROMA: a robust ICA-based strategy for removing motion artifacts from fMRI data. *NeuroImage*. 2015;112:267–277. <https://doi.org/10.1016/j.neuroimage.2015.02.064>.
- Rokem A, Takemura H, Bock AS, Scherf KS, Behrmann M, Wandell BA, Fine I, Bridge H, Pestilli F. The visual white matter: the application of diffusion MRI and fiber tractography to vision science. *J Vis*. 2017;17(2):4. <https://doi.org/10.1167/17.2.4>.
- Umarova RM, Saur D, Schnell S, Kaller CP, Vry MS, Glauche V, Rijntjes M, Hennig J, Kiselev V, Weiller C. Structural connectivity for visuospatial attention: significance of ventral pathways. *Cereb Cortex*. 2010;20(1):121–129. <https://doi.org/10.1093/cercor/bhp086>.
- Wang L, Mrcuzek RE, Arcaro MJ, Kastner S. Probabilistic maps of visual topography in human cortex. *Cereb Cortex*. 2015;25(10):3911–3931. <https://doi.org/10.1093/cercor/bhu277>.
- Zhang X, Manley CE, Micheletti S, Tesic I, Bennett CR, Fazzi EM, Merabet LB. Assessing visuospatial processing in cerebral visual impairment using a novel and naturalistic static visual search task. *Res Dev Disabil*. 2022;131:104364. <https://doi.org/10.1016/j.ridd.2022.104364>.